

# San Bernardino Wildland Fires

Assessing the Conditions of Pre-Fire and Post-Fire Vegetation in San Bernardino  
California with NASA Earth Observations

Spring 2025 | California – JPL  
April 4th, 2025

**Authors:** Sofia Ingersoll (Analytical Mechanics Associates), Samea Derrick (Analytical Mechanics Associates), Shilpa Kannan (Analytical Mechanics Associates), Darcy J. Tate (Analytical Mechanics Associates)

**Abstract:** Our team investigated a case study in San Bernardino, CA to understand prescribed (“Rx”) burning, namely how the Angelus Oaks Understory Prescribed (AOU Rx) Burn protected urban development from the spread of the Line Fire in 2024. Our team partnered with the U.S. Forest Service and the San Bernardino Valley Municipal Water District, who are responsible for conducting prescribed burns and maintaining public safety via land management. Using NASA Earth observation data—International Space Station (ISS) Earth Surface Mineral Dust Source Investigation, ISS Ecosystem Spaceborne Thermal Radiometer Experiment on Space Station, Harmonized Landsat Sentinel-2, and Uninhabited Aerial Vehicle Synthetic Aperture Radar—our team collected data from November 2023 through March 2025 to contextualize the vegetation conditions for the AOU Rx Burn and the Line Fire. To assess the landscape changes over time, we tabulated vegetation indices: canopy water content, evaporative stress index, water use efficiency, evapotranspiration, normalized differenced vegetation index, enhanced vegetation index, and soil burn severity. Comparison of the pre- and post-fire landscape conditions revealed more stable vegetation recovery rates for the prescribed burn in a shorter time span. The wildfire had a 0.003 larger significant decrease in the median Enhanced Vegetation Index overtime when compared to the AOU Rx burn (adjusted  $R^2 = 0.51$ , p-value < 0.05\*\*). Our evidence indicated the AOU Rx Burn may have served as a natural break and protected the nearby urban area from the Line Fire flames.

**Key Terms:** San Bernardino, wildland fires, prescribed burn, time series, risk, USDA, satellite data

**Advisors:** Dr. Madeleine Pascolini-Campbell (NASA Jet Propulsion Laboratory, California Institute of Technology), Dr. Karen An (NASA Jet Propulsion Laboratory, California Institute of Technology), Megan Ward-Baranyay (San Diego State University), Benjamin Holt (NASA Jet Propulsion Laboratory, California Institute of Technology)

**Lead:** Caroline Baumann (California – JPL)

## 1. Introduction

In the past decade, Southern California has become a hotbed for destructive, out-of-control wildfires (Donovan et al., 2020). These fires spread quickly because of shifting climatic conditions and available fuel. With hotter, dryer summers, gusty winds, and organic material covering the ground, a single spark can set entire counties ablaze. One area that is particularly at risk for wildland fires is San Bernardino County, which is home to approximately two million people and encompasses the San Bernardino National Forest (San Bernardino County, n.d.). This region can be characterized as the wildland urban interface (WUI) – the zone where regions of human development and structures meet vegetative fuels – a region that has also increased in area in recent decades. San Bernardino's residents are heavily impacted by wildland fires because of their proximity to the forest. A 2008 case study of San Bernardino National Forest residents revealed that 87.6% of participants experienced road closures, 67.7% previously evacuated their homes, and 69.7% reported shut off or reduced power (Cvetkovich & Winter, 2008). This pattern of mass displacement is cause for concern and calls for more resources to be committed to fire analysis.

One of the main factors of wildland fires is the available fuel, and there are methods to mitigate the risk of dried organic material compounding these natural disasters. One of the primary solutions is prescribed burns, which are controlled fires intentionally created by agencies to remove excess fuel (Miller et al., 2020). Prescribed burns serve as an effective method to build ecosystem resilience by reducing fuel accumulation, improving ecosystem health, and preventing large-scale burns (U.S. Department of Agriculture, Forest Service, 2023).

We set out to understand the efficacy of prescribed burning with a natural case study: the Line Fire and the Angelus Oaks Understory (AOU) Prescribed Burn (Rx; Figure 1). The AOU Rx burn was active from April 30 – May 3, 2024, and the Line Fire burned from September to December of 2024. Since the Line Fire halted at the area of the prescribed burn, we wanted to investigate how fuel load and water content impacts fire spread and vegetation recovery. We sought to understand the direct impacts of the AOU Rx burn through pre- and post-fire landscape analysis using synergies between different satellite sensors.

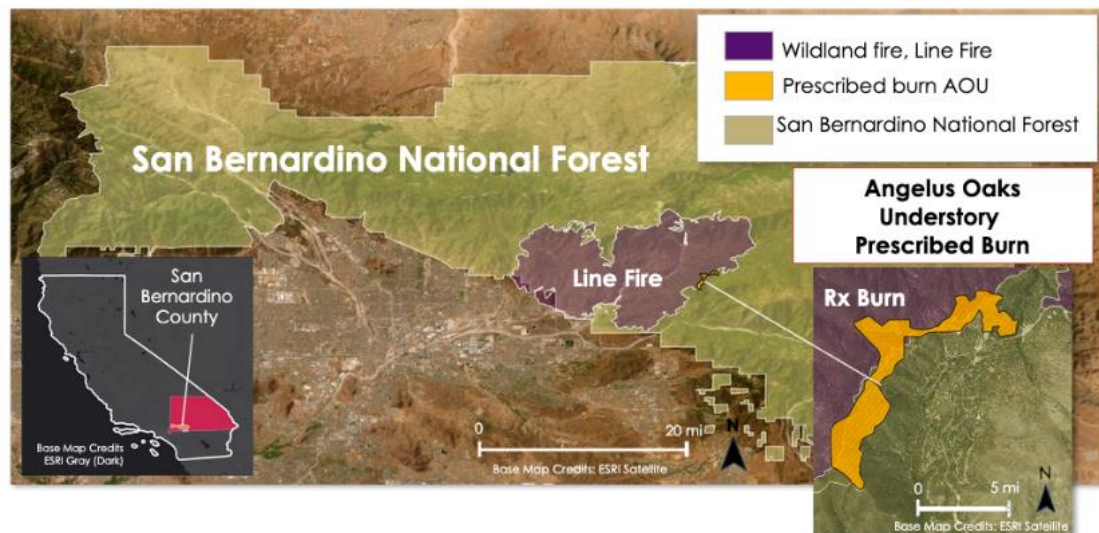


*Figure 1.* Highlighted study area contains the extents of the Line Fire and the Angelus Oaks Understory Prescribed Burn, and all of San Bernardino County in California, United States.

We partnered with the United States Department of Agriculture (USDA), United States Forest Service, Wildland Fire Management Research & Development (1); the USDA, United States Forest Service, San Bernardino National Forest (2); and the San Bernardino Valley Municipal Water District (3) to provide pre- and post-fire analysis to impact mitigation and land management strategies between November 2023 to March 2025. Our research informed partners of before and after fire fuel loads, vegetation health, and burn

severity throughout the fire extents. We also collaborated with the Institute for Watershed Resiliency (IWR, 4) and CSU Northridge, Center for Geospatial Science & Technology (5) for additional support (Table 1).

Table 1.  
*Project Partners*

| Partner | Existing Strategy and Involvement  |
|---------|--|
| 1       | An interagency program that prioritizes fire protection with fire prediction technology and risk management tools (U.S. Department of Agriculture, Forest Service, 2021). They lacked quantification of burned areas that impacted mitigation and land management strategies. Our project served as an outline for land use and land cover analysis in pre-fire and post-fire landscapes to apply throughout California. |
| 2       | A federal agency that manages San Bernardino National Forest ( <i>Fire management</i> , n.d.). Their environmental decision for forest management relied on moisture readings of vegetation to treat fire-prone areas. We provided moisture readings of land cover before and after fires, which may impact land management practices.   |
| 3       | A regional agency responsible for the water supply of San Bernardino Valley that includes fire protection services ( <i>About us</i> , n.d.). They allocate and manage water services and work to better understand the erosion and runoff of fires and how they impact water quality. We supported the agency's understanding of how fires impacted the landscape with land cover change figures and analysis.          |
| 4       | A research institute with community-university partnerships that study issues surrounding water resources ( <i>Institute for Watershed Resiliency</i> , n.d.). IWR studies fire impacts on dams and water for public partners and potential policy changes. We highlighted physiological and urban effects of fires on land, water, and infrastructure so they could incorporate them into their research.               |
| 5       | A research center focused on geospatial technology with projects regarding pre-fire planning and management monitoring ( <i>Center for Geospatial Science and Technology</i> , n.d.). We provided fuel maps and land cover time series for their scientific communication and future work.   |

Successful studies done previously to assess pre- and post-fire landscape conditions include emphases on resource disparities, vegetation classifications, and conditions using Earth observation data from ECOSystem Spaceborne Thermal Radiometer Experiment on Space Station (ECOSTRESS), Harmonized Landsat Sentinel-2 (HLS), and Earth Surface Mineral Dust Source Investigation (EMIT; Zhu et al., 2024; Roteta et al., 2021). Deeper inspection into the vegetation water content using these data in tandem with Uninhabited Aerial Vehicle Synthetic Aperture Radar (UAVSAR), and Landscape Fire and Resource Management Planning Tools (LANDFIRE) provided a well-rounded approach to determining fuel availability and post-fire regrowth levels (Lopez-De-Castro et al., 2022). NASA employed these data in similar natural wildfire case studies including the Station Fire, Colby Fire, San Gabriel Complex Fire, La Tuna Fire, and Bobcat Fire (Gabbert, 2021).

Considering these approaches and their insights, we emphasized identification of fire-fuel load changes since assessments of fuel load accumulation under evolving climate conditions provide insights into the unprecedented frequency and prevalence of fire in Southern California (Keifer et al., 2006; van Wagtendonk et al., 1998). We used multiple satellite missions to more fully understand prescribed burn efficacy. From thermal infrared (ECOSTRESS) we determined vegetation temperature and related it to water use and water stress; from visible to shortwave infrared imaging spectroscopy (EMIT) we assessed canopy water content, and from Landsat data we characterized land cover type and burn severity. Using different sensors allowed us to see a wide range of spatial and temporal resolutions and capture short- and long-term fuel changes.

## 2. Methodology

### 2.1 Data Acquisition

To accomplish this analysis, we utilized a variety of remote sensing tools. We used data from ECOSTRESS and EMIT to assess resource disparities and delineate various vegetation conditions (Zhu et al., 2024). We also used HLS Surface Reflectance 30m data to detect pre- and post-fire changes in land cover classifications (Roteta et al., 2021). Additionally, we used UAVSAR to validate soil burn severity.

We gathered LANDFIRE information to understand fuel availability and track post-fire regrowth levels (*About LANDFIRE*, n.d.). LANDFIRE, or Landscape Fire and Resource Management Planning Tools, is a wildland fire management dataset from the U.S. Department of the Interior and the U.S. Department of Agriculture Forest Service. LANDFIRE developers created vegetation cover and height layers by assigning pixels values to vegetation types based on Forest Inventory and Analysis training data. They created the classification type class by compositing seasonal scenes and assigning classifications for each data type. For surface and canopy fuel, developers manipulated vegetation type, cover, height, and disturbance layers with a linear regression analysis for canopy base height and equations for crop cover and crop height (U.S. Department of the Interior, U.S. Geological Survey, 2023). Table 2 showcases the location where LANDFIRE and each other data set was acquired.

Table 2.  
*Earth Observation Sensor Data Information*

| Dataset       | Level   | Spatial Res. | Temporal Res.   | Years Available         | Acquisition Platform   | Search Attributes   |
|---------------|---------|--------------|-----------------|-------------------------|--|---|
| ISS ECOSTRESS | 3L & 4L | 70 m         | Periodic        | 2022–2024               | Application for Extracting and Exploring Analysis Ready Samples (AppEEARS)                 | Evapotranspiration Instantaneous and Daytime L3 Global, Evaporative Stress Index PT-JPL Instantaneous L4 Global, Water Use Efficiency Instantaneous L4 Global, L3/L4 Ancillary Data Quality Assurance (QA) Flags;<br><b>File Format:</b> GeoTIFF, <b>Projection:</b> Geographic |
| ISS EMIT      | 2A      | 60 m         | Periodic        | 2022–2025               | EarthData Search   | EMIT L2A Surface Reflectance<br><b>File Format:</b> GeoTIFF, <b>Projection:</b> Geographic  |
| HLS           | 3L      | 30 m         | 8 days          | 2015–2025               | AppEEARS   | Band Layers: B02, B03, B04, B05, B06, B07;<br><b>File Format:</b> GeoTIFF, <b>Projection:</b> Native  |
| UAVSAR        | 2L      | 7 m          | Sporadic        | 2015–2021 and 2023–2024 | Alaska Satellite Facility Distributed Active Archive Center (ASF DAAC) generated.py script | L-band, POL, Full polarization, Ground Project Complex, multi-look complex, Slope, GEOTIFF Height File, Metadata<br><b>File Format:</b> .zip, .mlc, .kmz, .hgt, .tiff, .ann<br><b>Projection:</b> Geographic  |
| LANDFIRE      | NA      | 30 m         | Every 1-2 years | 2023                    | LANDFIRE.gov   | All attributes for all available years<br><b>File Format:</b> GeoTIFF, <b>Projection:</b> Geographic  |

The available dates associated with each dataset relate specifically to its availability within our study area. The temporal range we inspected was between November 2023 to March 2025 (Figure 2). This period includes the largest breadth of available data for our natural case studies across all sensors. We applied spatial filters

for the San Bernardino National Forest (SBNF), the Line Fire, and the Angelus Oaks Understory (“AOU”) Rx Burn perimeters when gathering data.

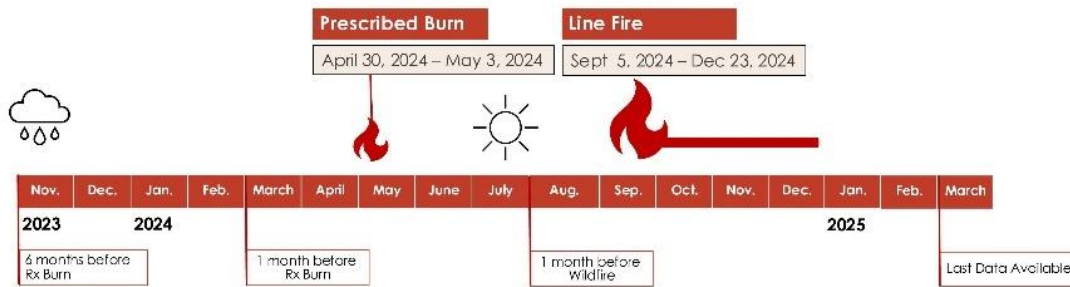


Figure 2. Study period timeline highlighting the prescribed burn, Angelus Oaks Understory Prescribed Burn (April–May 2024), and wildfire, Line Fire (October–December 2024).

When acquiring data, we sought data before and after both fires. For each fire, we prioritized data six months and one month before the burn to understand how the baseline vegetation and fuel loads existed at ignition and how extraordinarily wet or dry seasons impacted the landscape. We collected multiple scenes after the fires to better understand how the landscape recovered. Since the wildfire was not fully contained until December 23, 2024, there is limited data availability post-Line Fire (Incident Information System, n.d.).

## 2.2 Data Processing

We applied different processing and analysis workflows for each of the sensor datasets using a combination of Python 3.12.8 and ArcGIS Pro 3.4.2. We relied on the NASA-designed scripts, which were hosted in various repositories. We developed maps to quantify water use trends using canopy water content, water use efficiency (WUE), evapotranspiration (ET), and evaporative stress index (ESI) to assess pre- and post-fire fuel conditions using ISS EMIT and ISS ECOSTRESS. To interpret and compare landscape changes between the two fire types, we tabulated normalized difference vegetation index (NDVI), enhanced vegetation index (EVI), and differenced normalized burn ratio (dNBR) using HLS.

### 2.2.1 Quantifying Vegetation Water Use Trends

To interpret terrestrial biosphere trends relating to water availability, we used the ISS ECOSTRESS sensor. This sensor contains pertinent information relating to how vegetation uses water (NASA Jet Propulsion Laboratory, n.d.). To process the ECOSTRESS data, we harnessed the ‘02\_Working\_with\_EMIT\_Reflectance\_and\_ECOSTRESS\_LST.ipynb’ script from NASA’s ‘VITALS’ repository (Land Processes Distributed Active Archive Center, 2024a). In this script, we manipulated Level 3 Tiled Evapotranspiration products, which were estimated from Level 2 Tiled Land Surface Temperature products and other inputs. Level 3 data are preprocessed, so we generated an evapotranspiration color ramp, visualized, and cropped the data. After running the script, we documented ET, WUE, and ESI.

To understand canopy water content throughout the study area, we used the ISS EMIT sensor. We used the ‘02\_Working\_with\_EMIT\_Reflectance\_and\_ECOSTRESS\_LST.ipynb’ and ‘03\_EMIT\_CWC\_from\_Reflectance.ipynb’ scripts from NASA’s ‘VITALS’ repository to manipulate the raw data. The first notebook accessed the raw ISS EMIT data, documented spectral information, applied a cloud mask, linked surface reflectance to wavelength, selected ten points to serve as a baseline for canopy water content, and exported the spectra and points in an Excel file (Land Processes Distributed Active Archive Center, 2024a). Then, we clipped the preprocessed EMIT data to the study area, first for the Line Fire, then for the prescribed fire, to provide side-by-side comparisons.

In the second script, we used the Beer-Lambert physical model data to estimate canopy water content (CWC) by using wavelength-dependent absorption coefficients of liquid water to identify absorption path lengths as a function of the absorption feature depth (Land Processes Distributed Active Archive Center, 2024b). We



estimated the path length of liquid water absorption by using a least squares inversion to minimize residuals between the Beer-Lambert physical model and our EMIT reflectance (Land Processes Distributed Active Archive Center, 2024a; Green et al., 2006). The algorithm works by modeling surface reflectance as a linear change in reflectance with respect to the wavelength. We then multiplied that linear change in reflectance by the spectral dependent absorption for water through their distinct path lengths. The Beer-lambert physical model assumes that the general spectral solar energy absorption effect of water within 850 – 1100 nm is proportional to its baseline reflectance (Green et al., 2006). Once we set up the equations to calculate water content, we imported our study area to calculate each included pixel and visualize the canopy water content.

### 2.2.2 Comparing Landscape Change by Fire Type

To tabulate the NDVI and EVI time series, we initially gathered these indices for the entire San Bernardino National Forest using the HLS data. We applied Equations 1 and 2 to calculate the NDVI and EVI indices respectively (Tucker, 1979). These equations collectively utilize the Near Infrared (NIR), Red, and Blue Bands.

$$\text{NDVI} = \frac{\text{NIR} - \text{Red}}{\text{NIR} + \text{Red}} \quad (1)$$

$$\text{EVI} = 2.5 * \frac{\text{NIR} - \text{Red}}{(\text{NIR} + 6 * \text{Red} - 7.5 * \text{Blue} + 1)} \quad (2)$$

We utilized HLS data to both calculate NBR (Normalized Burn Ratio) represented as Equation 3 as a method of distinguishing burned regions, and dNBR (Difference Normalized Burn Ratio) represented as Equation 4 to reflect burn severity as a change between pre-fire and post-fire environments (United Nations Office for Outer Space Affairs UN-SPIDER, n.d.). These equations utilize the second Short-Wave infrared band (SWIR2).

$$\text{NBR} = \frac{\text{NIR} - \text{SWIR2}}{\text{NIR} + \text{SWIR2}} \quad (3)$$

$$\text{dNBR} = (\text{pre-fire})\text{NBR} - (\text{post-fire})\text{NBR} \quad (4)$$

For classification of soil burn severity, we used the ‘burn\_severity.ipynb’ United Nations Platform for Space-based Information for Disaster Management and Emergency Response (UN-SPIDER) script to calculate the dNBR and NBR indices (UN-SPIDER, 2018). Once we completed the calculation for the indices, we transformed the final data from an array back to a GeoTIFF projected raster.

From the NASA-JPL code repository ‘uavsar-wildfire-rtc,’ we leveraged Python scripts to process the raw UAVSAR data (Simard et al., 2016; California Institute of Technology, 2023). We used the script ‘RTC\_notebook.ipynb’ to apply the radiometric terrain correction (RTC). To complete the RTC calculation, we used the file types .mlc, .hgt, and .ann to produce .hdr files. This was to account for backscatter estimates and eliminate geometric distortions and terrain within the radar shadow (An et al., 2024). We used the polarization horizontal-vertical (HVHV) to highlight volume scattering from forest canopy (NASA EarthData, n.d.). We converted the horizontal-vertical values to decibel units, and produced an HV difference (or log ratio) map to provide insights into post-fire conditions for vegetation and soil burn severity (An et al., 2024).

## 2.3 Data Analysis

### *2.3.1 Quantifying Vegetation Water Use Trends*

To contextualize our study area, we visualized LANDFIRE data pertaining to existing vegetation classes, historical land cover changes, and canopy cover percentages (Figures A.1, A.2, & A.3). Then we were able to move to CWC from EMIT. While CWC is often limited by vegetation type, in general higher CWC points to healthier and more fire-resistant vegetation (Martin et al., 2018). ISS EMIT had data available pre-fire in 2023, which helped understand the context of the landscape in regard to fire-resistance. To understand the landscape statistically, we created histograms for the Line Fire extent and the AOU extent (Figure B.2). We calculated the mean, median, minimum/maximum, and standard deviation in ArcGIS Pro and created histograms to visualize the distribution throughout the fire perimeters. We exported the histogram results from ArcGIS Pro to Excel to revisualize for further clarity. Because both fire extents had bimodal distributions, we did not apply any transformations to avoid data censorship. We also created maps to visualize the distribution of CWC throughout the fire extent.

Utilizing ECOSTRESS's ET, ESI, and WUE data, we created pre- and post-fire maps for both fires. We produced these maps by combining raster files into a composite image from time windows of interest for each variable (Figure 2). To further understand fires' impact on vegetation we synthesized histograms for WUE and ESI data 3 months prior and 3 months post-fire, for each fire (Figure B.3). We visualized this change between data by calculating the difference between the pre- and post-fire rasters. Overall, we conducted this process to assess vegetation stress and primary productivity before and after the fires.

### *2.3.2 Comparing Landscape Change by Fire Type*

To compare the prescribed burn and wildfire over time, we clipped the NDVI and EVI data using the fire perimeters, collecting the values and associated dates into a dictionary. We conducted time series analysis using ordinary least squares (OLS) regressions on the indices for each fire and visualized the values density distribution. Since our aim was to better comparatively understand the rate of vegetation recovery, we quantified time's influence on the vegetation indices within the two fire areas (Jamali et al., 2015).

We used the processed dNBR data to develop maps for both fires for further visual interpretation and comparison. We assessed the data against elevation topography and vegetation type. To quantitatively compare the difference burned between the two fires, we plotted bar and dumbbell graphs that provide estimations for hectares burned in each of the regions by burn severity type.

## **3. Results**

### ***3.1 Quantifying Vegetation Water Use Trends***

#### *3.1.1 Canopy Water Content & Pre-fire Landscape Context*

To contextualize results, we used LANDFIRE data to understand the landscape in 2023. When analyzing the historical vegetation departure, most of the Line Fire's extent was classified as 'Very High' or 'Drastically Different' than the historical vegetation precedent, indicating these areas contained a surplus of available fuel compared to previous conditions. The AOU area was categorized with 'Moderate to Low' changes to normal vegetation levels. This is likely related to the regular prescribed burns the US Forest Service conducted since 2010. We also leveraged LANDFIRE to understand historical tree cover percentages within our study region. Tree canopy cover often indicates a higher level of water content, which can indicate how susceptible an area is to fires. Before 2023, approximately half of the Line Fire extent consisted of moderately dense tree cover of 40–60%, with the remaining extent consisted of different vegetation types or barren soil (Figure A.1, A.3). Considering the AOU perimeter has undergone regular prescribed burning since 2010, this area was more evenly populated with 30–50% canopy cover (US Forest Service, n.d.), and has far less areas with no canopy cover. This means there was likely less dry fire fuel load within the prescribed burn extent.

We collected ISS EMIT sensor data to visualize the water use trends using a pre-fire map. Water content ranged from 0.05 to 0.35 g/cm<sup>2</sup> throughout the fire extents. The water content was more normalized within the AOU perimeter, likely due to its smaller size and regular Rx burn treatments. We observed correlation between CWC and the type of vegetation, where some vegetation types were able to store more water than others. We were unable to conclude how canopy water content changed after the fires, since no after-fire data

were available. However, it is still helpful to compare the distribution of high and low CWC before the prescribed and Line Fire alongside the historical LANDFIRE data (Figure 3).

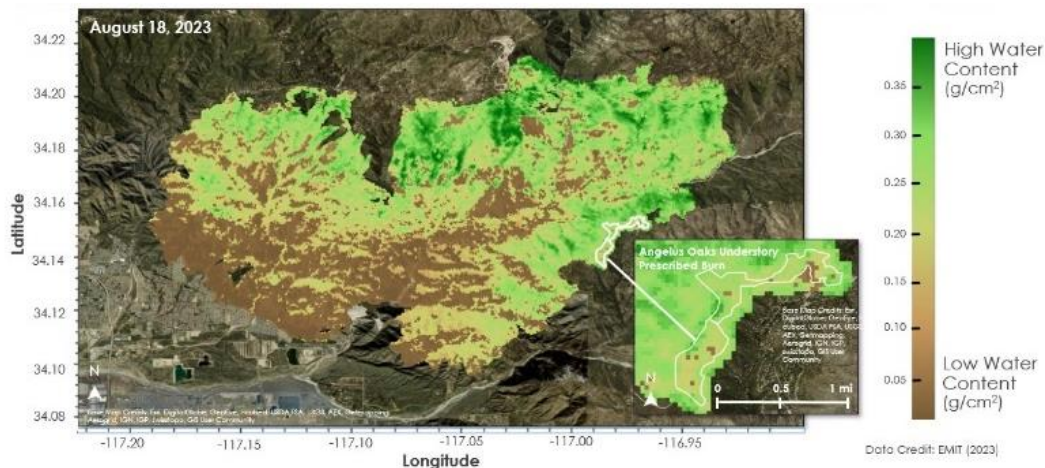


Figure 3. Canopy Water Content (CWC) estimated with ISS EMIT surface reflectance values in Line Fire and AOU Burn extents.

Histograms for the Line Fire and AOU Rx Burn show different distributions (Figure B.2). In the Line Fire extent in 2023, the CWC has a distinct bimodal distribution with peaks around  $0.15 \text{ g/cm}^2$  and  $0.48 \text{ g/cm}^2$  and a range of  $0.59 \text{ g/cm}^2$ . When cross-referenced with LANDFIRE classification data, areas of high water content usually fall under the vegetation class of ‘Open Tree Canopy.’ Areas with low water content tend to fall in the ‘Shrubland’ vegetation class, which have lower CWC capacities. The extent of the AOU Rx Burn was more normalized and had a much smaller range of  $0.27 \text{ g/cm}^2$ . There were a few areas of distinctly low water content, which correlates to shrubland. The median of the Line Fire was  $0.41 \text{ g/cm}^2$  while the median for the AOU Rx Burn was  $0.20 \text{ g/cm}^2$  meaning that overall, the Line Fire had higher water content throughout. Having higher water does not necessarily mean that an area is less fire resistant. Because the Line Fire’s extent was much larger than the AOU Rx Burn area, the water content varied widely, so even areas of high-water content were subject to wildland fire destruction since dry fuel load scattered the area. This allowed the Line Fire to travel widely throughout the San Bernardino National Forest. The prescribed burn’s more normalized water content lent less opportunity for wide-scale burns because it lacked dry fuel load throughout. While ISS EMIT data set up expectations of fire behavior, the limited data available meant that before and after comparisons were not possible.

### 3.1.2 Evaporative Stress Index (ESI)

We utilized the ISS ECOSTRESS sensor to assess ESI. ESI denotes the amount of water stress vegetation is experiencing due to reduced water availability and is a ratio between evapotranspiration and potential evapotranspiration. A higher ESI indicates low water stress while a lower ESI indicates high water stress. We visualized ESI pre- and post-fire for both fires as histograms, the change in data trends was inverse between the two fire events (Figure B.3). The Line Fire caused ESI to shift from a bell curve to a bimodal distribution, with data peaks at low and high ESI. The AOU fire showed the opposite effect, where pre-fire ESI was a bimodal distribution at the high and low extremities of values, and post-fire ESI shifted to a bell curve above the median 0.5. This difference demonstrates that the AOU burn smoothed out vegetation ESI while the Line Fire exacerbated the extremities. The right most peak in ESI post Line Fire may be a result of re-growing invasive vegetation that outcompetes surrounding vegetation. Invasive grasses frequently repopulate burned land quicker than native species, which can in turn increase fire fuel loads quicker. Additionally, the re-growing of vegetation, whether invasive or not, could inaccurately represent the historic or expected vegetation of the area (Fusco, 2019). This is of concern regarding preservation and restoration efforts. It should also be considered that unburned vegetation may have influenced this data. The greater ESI shown



with the AOU fire may be a result of this unburned vegetation due to its low intensity. Lower intensity prescribed burns could allow for greater ESI values to persist. This data was normalized to limit the effect that area had on the distribution of the data. However, the vegetation type present in the region was not considered when quantifying ESI. As such, differing vegetation could have affected these results.

### 3.1.3 Water Use Efficiency (WUE)

To further understand vegetative stress, we extracted WUE from ECOSTRESS. WUE represents how efficiently plants use water for photosynthesis. WUE estimates the rate of carbon uptake per unit of water lost. A WUE closer to 0 denotes lower carbon uptake efficiency and less healthy vegetation, while a higher WUE signifies increased carbon uptake. We used this to observe the impact both fires had on the efficiency of vegetative primary productivity. We visualized WUE pre- and post-fire for both fires as histograms (Figure B.3). The Line Fire had an overall decrease in WUE. While there was an increase in pixel density at 10 WUE, these may be outliers. This is because the density distribution of the remaining pixels was minimally affected. Regarding the AOU fire, there was minimal change. We considered seasonal effects on vegetation, normalized the data, and omitted values signifying barren soil. The minimal change observed may be the result of a collection error, lower sample size, or inaccurate visualization; however, it is likely that the AOU fire had no effect on WUE. The Line Fire ultimately had a greater negative impact on WUE than the AOU prescribed burn. In turn, the AOU prescribed burn had little to no impact on the vegetation water stress, further supporting the use of this land management tool. The variations we saw between vegetation water use trends within the prescribed burn and wildfire areas led us to question how the landscape greenness was affected over time by the Line Fire. To quantify these changes and further explore the previous water use trends of the local vegetation, we inspected NDVI and EVI.

## 3.2 Normalized Difference Vegetation Index (NDVI) & Enhanced Vegetation Index (EVI)

### 3.2.1 Normalized Difference Vegetation Index (NDVI)

We calculated NDVI to describe vegetation health by quantifying the amount of green in plants. EVI was tabulated to provide greater insights related to canopy coverage and vegetation greenness in these thicker vegetative areas because the approach is more sensitive to vegetation density and canopy background noise. To gauge immediate vegetation impacts we visualized the changes in NDVI greenness for the Line Fire one month prior, as well as one- and three-months post-fire. Our investigation displayed a dramatic change in vegetation greenness caused by the Line Fire near the end of 2024. Before the wildfire, in August 2024, greenness was high, closer to 1, which indicated widespread, healthy vegetation (Figure 4). One month following the wildfire, January 2025, a distinct extent of the Line Fire dropped below 0, nearing -1, indicating barren soil or dead vegetation (Figure 4). When we evaluated the trends in NDVI over time, there were no significant relationships. Our analysis of the changes within the most barren regions of the Line Fire burn scar from January 2025 to March 2025 indicated potential vegetation with greater wildfire resiliency.

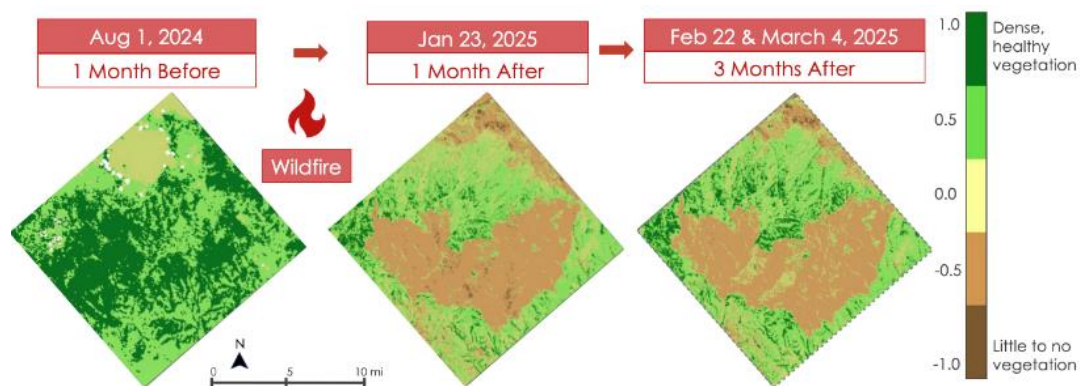


Figure 4. NDVI Landscape Greenness Trends in Line Fire extent from September 5 – December 21, 2024. Pre- and post-Line Fire NDVI “vegetation greenness” in San Bernardino National Forest, San Bernardino, CA (HLS 2024–2025).

Minor recovery in the areas identified as barren soil (dark brown) was observed in late February and early March of 2025 (Figure 4, C.1, C.2). Reflecting on the 2023 LANDFIRE vegetation classifications, these swiftly recovering areas were associated with a mixture of sparse tree canopy, open tree canopy, shrubland, and sparse vegetation. This evidence suggests vegetation of this classification type may have increased resiliency resulting from shorter recovery times following wildfires. However, deeper considerations for the landscape topography, plant seasonality, and comparative levels of burn severity are needed to validate these claims. It is important to note that NDVI does have some limitations and does not work as well in densely vegetated areas (Rhew et al., 2011). As revealed in the LANDFIRE changes historical vegetation density and EMIT pre-fire canopy water content trends, the Line Fire region was highly populated with dense canopy coverage (Figures A.1, A.2, A.3, B.1). For this reason, we also computed the EVI.

### 3.2.2. Enhanced Vegetation Index (EVI)

By employing EVI, we collected greater insights into canopy greenness in more densely vegetated areas. Similar to NDVI, we witnessed a significant decrease in landscape greenness following the wildfire. The area prior to the fire, in August 2024, was considered dense and healthy with a range of ~2 (Figure 5, C.3). Following the wildfire, in January 2025, we observed a large and distinct burn scar area, indicating lowered vegetation density considerably and in some cases to the point bare soil, a 0 or less (Figure 5). For consistency, we also compared the EVI median values of both the fires overtime. Using a simplified regression analysis, Eq. 2, we found a significant ( $p\text{-value} < 0.05^{**}$ ) decreasing relationship in dense vegetation greenness for both fire areas as time continued (Figure 5, C.4).

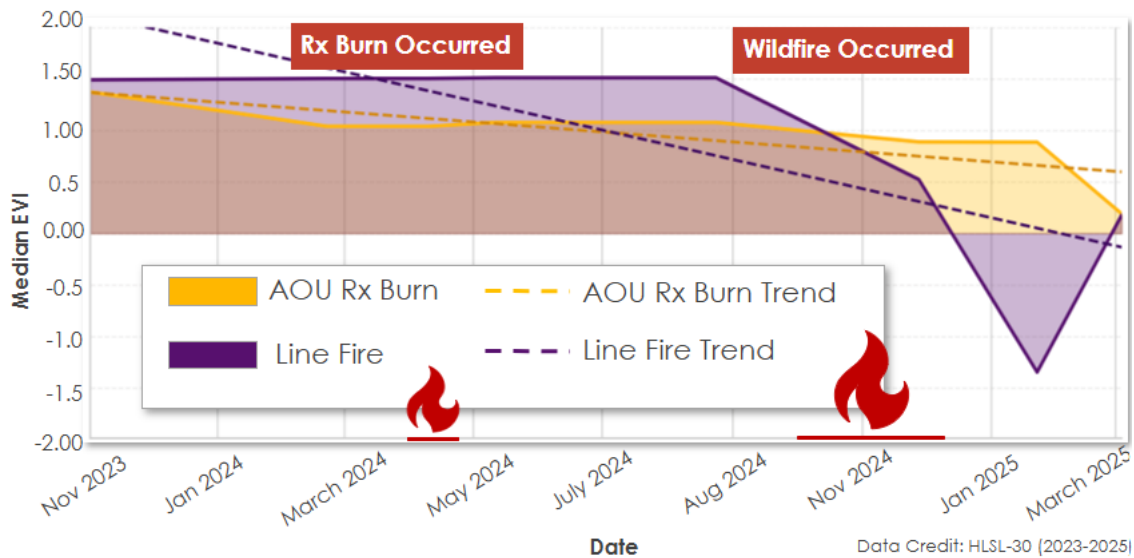


Figure 5. Enhanced vegetation index time series regression analysis on pre- and post-fire conditions for the Angelus Oaks Understory Rx Burn (gold) and the Line Fire (purple) (HLS 2024–2025).

When comparing the wildfire's median EVI greenness trends overtime (shown in purple) to the prescribed burn greenness trends (displayed in gold) we observed a rapid decrease in greenness within the wildfire area following the start of the Line Fire on September 5, 2024 (Figure 5). The wildfire median EVI exemplifies the drastic drop in greenness immediately following ignition. A significant ( $p\text{-value} < 0.05^{**}$ ) decrease of  $0.0046 \pm 0.002$  in median EVI was predicted for a single unit increase in time with an adjusted  $R^2$  of 0.51. The

wildfire time series highlighted longer recovery times required to return to the pre-fire levels of vegetation greenness. In the 3 months following the Line Fire, we observed vegetation in this region had not yet recovered to similar levels prior to the wildfire (Figure 5), indicating a slower recovery rate compared to the Rx burn area.

However, the prescribed burn median EVI remained relatively consistent over time with a shallow dip around the time of the prescribed burn (Figure 5). The vegetation has somewhat steady recovery rates, with a significant ( $p\text{-value} < 0.05^{**}$ ) decrease of 0.0016 in median EVI for a single unit increase in time for an adjusted  $R^2$  of 0.58. Throughout the time series, the AOU Rx burn demonstrated stable vegetation trends for this fire type, bolstering evidence of its ability to reduce fire-fuel availability without devastating the landscape. We considered this behavior to be supporting evidence of the benefits of regular Rx burns in this area.

It is important to note there were limitations to this regression analysis above due to the time restrictions of this project. This analysis may be subject to omitted variables bias due to lack of consideration for interacting relationships (Carelton, n.d.). Our model was not exogenous because we neglected to include variables such as precipitation, which in turn are influenced by seasonality, or in this case, time. The purpose of this analysis was to generally interpret immediate changes in the vegetation greenness following exposure to different fire-types. Greater contextualization of the landscape and its associated burn severities are required to draw any full conclusions. To better understand how the intensities of the fire-types differed, we chose to explore the difference in normalized burn ratios.

### ***3.3 Soil Burn Severity Classifications***

#### ***3.3.1 Differenced Normalized Burn Ratio (dNBR)***

Applying the insights we gained for both vegetation water uses and greenness trends, we investigated how these factors influenced the landscape burn severity for each fire. The colors within the Line Fire dNBR map on the left indicate the various levels of severity, with yellow defining unburned and black defining high burn severity (Figure 6). The map displays higher levels of burn severity throughout the region compared to the AOU prescribed burn (Figure D.1). Through visual comparison against elevation levels, we identified that areas with higher slopes tended to have higher severity burns (Figure 6, D.2). This is likely due to how pre-heated fuel from uphill burns cause fire to spread quickly and how many of the south facing mountains in the Line Fire have more exposure to sunlight and are more likely to ignite (Northwest Fire Science Consortium, 2017). On the other hand, areas that experienced no or low severity burns tended to surround creeks or roads, which served as a natural barrier for fire spread. Like the Line Fire, the AOU Prescribed Burn's higher severity burns did not spread past regions with high elevation. It experienced much lower burn severity, likely because the burn was controlled and had minimal fuel access. To validate these measurements, we leveraged UAVSAR to confirm the extent of the soil burn severity following the Line Fire (Figure D.4, D.5).

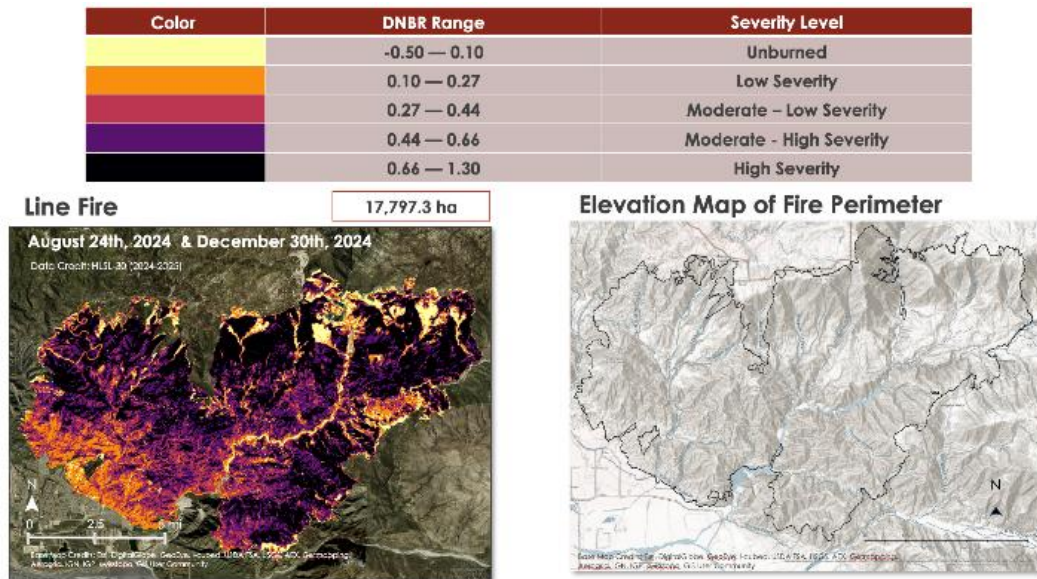
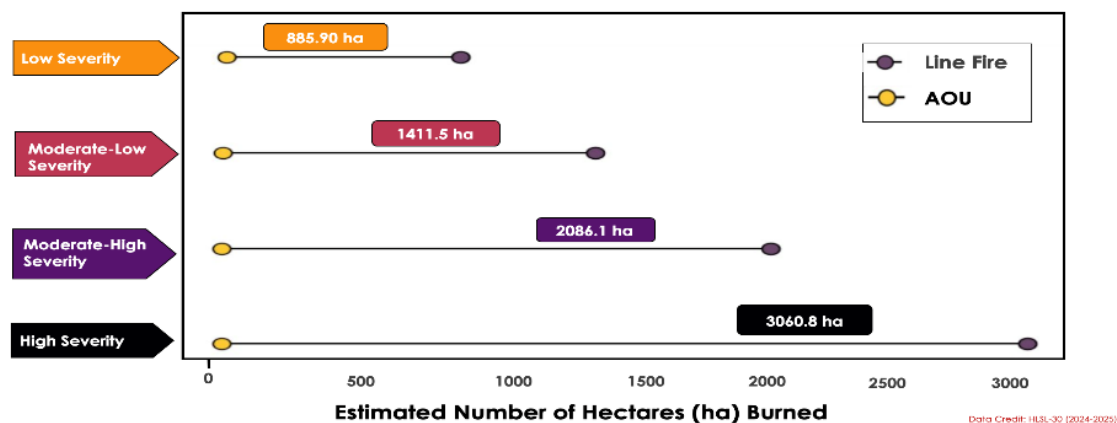


Figure 6. Line Fire Categorized by Soil Burn Severity illustrating dNBR (left) and elevation in San Bernardino National Forest, San Bernardino, CA (HLS 2024–2025; right).

We identified visual links between burn severity classification and existing vegetation classes within the Line Fire and AOU regions. Within the Line Fire, areas that were sparsely vegetated or shrubland tended to be associated with low or moderate-low burn severity, while regions with sparse tree canopy tended to fall under moderate to high severity. Regions with open tree canopy aligned with burn areas classified as high severity. The AOU Prescribed Burn did not have any clear associations between vegetation class and burn severity levels.

We also compared the estimated hectares of burned area by burn severity levels for each fire. In total, the Line Fire resulted in 17797.3 hectares burned, in contrast to the AOU's 80.9 hectares (Figure 6). The largest difference was in high severity burn levels at 8000 hectares, while the lowest is low severity at over 2000 hectares. Within these classifications, 76% of the AOU's burn scars were low severity, while this only consisted of 12% of the Line Fire's burns (Figure 7). Additionally, 40% of the Line Fire's burns were classified as High Severity, while none were identified in the AOU (Figure 7, D.3). As such, the Line Fire resulted in significant amounts of burn disturbance when compared against the AOU prescribed burn, which consequently had much lower severity controlled-burns that allow for healthy regrowth patterns.



*Figure 7. Comparing Difference in Estimated Hectares within the Line Fire (purple) and AOU Prescribed Burn (gold) fire perimeters by Burn Severity Classification in San Bernardino National Forest, San Bernardino, CA (HLS 2024–2025).*

We utilized dNBR to develop a better understanding of how topography, vegetation classification, and fire-type contributed to different levels of burn severity and hectares burned. When measuring area using HLS dNBR data, there was no pre-processing done before the calculation of hectares due to time restrictions and land area file resource availability. This hindered accurate assessments of area per pixel, and we instead opted to utilize area estimations using a scalar factor against pre-existing information of each region’s overall size.

## 4. Conclusion

All in all, harnessing a wide variety of Earth observation data allowed us to convey the comparative impacts of wildfires vs prescribed burns on the landscape. We provided evidence to support the effectiveness of consistent prescribed burns in the San Bernardino National Forest AOU area to reduce available fire-fuel loads. This evidence supports the sentiment that reduced fire-fuel loads decrease the risk of wildfires and preventing wildfires from growing larger and spreading to nearby urban areas. In the case of the Angelus Oaks Understory Rx Burn, the prescribed burn protected nearby urban areas and reduced the risk of wildfire devastation caused by the Line Fire.

### 4.1 Feasibility & Partner Implementation

Our study emphasized the need for NASA EO tools such as NASA-ISRO Synthetic Aperture Radar (NISAR) and Surface Biology and Geology (SBG) that have greater availability and shorter data processing release times (NASA JPL, n.d.). Our data was subject to some limitations, as some sensors had sporadic revisit times, varied greatly in resolution, and were dependent on minimal cloud coverage (Figure E.1). The range in resolution may pose some challenges if combined for future projects. However, each observation tool provided insights into landscape conditions at key periods. Our evidence indicated the AOU Rx Burn may have served as a natural break and protected the nearby urban area from the Line Fire flames (2024). To further explore resiliency in post-fire vegetation, different case studies or the use of extended study periods may provide more evidence to support our findings.

The San Bernardino National Forest is home to several watersheds, reservoirs, and the Seven Oaks Dam (Figure A.1, Figure E.2). Our partners, the U.S. Forest Service and the San Bernardino Valley Municipal Water District, expressed an interest in expanding our project to better understand the implications on local water supplies caused by these considerations. Using Earth observations, other impacts caused by wildfires may be studied, such as analyzing changes in soil composition, sedimentation trends that may lead to run-off into water supplies, and negative impacts to dams. We recommend the use of ISS EMIT to study these variables to gain a greater understanding of the landscape changes.

## 5. Acknowledgements

We would like to say thank you to all the wonderful individuals who helped make this project possible:

**JPL Node Lead:** Caroline Baumann

**Science Advisors:** PhD Candidate Megan Ward-Baranyay (SDSU), Dr. Karen An (NASA JPL, CalTech), Dr. Madeleine Pascolini-Campbell (NASA JPL, CalTech), Benjamin M Holt (NASA JPL, CalTech)

**Partners:** Kristen Allison (USDA, Wildland Fire Management R&D), Lauren Blake (USDA, San Bernardino national forest), Chris Jones (San Bernardino Municipal Water District), Dr. Jennifer Alford (CSUSB, Institute for Watershed Resiliency) Dr. Danielle Bram (CSUN, Center for Geospatial Science & Technology)



This material contains modified Copernicus Sentinel data (2024), processed by ESA.

Any opinions, findings, and conclusions or recommendations expressed in this material are those of the author(s) and do not necessarily reflect the views of the National Aeronautics and Space Administration.

This material is based upon work supported by NASA through contract 80LARC23FA024.

## 6. Glossary

**AOU** - Angelus Oaks Understory

**AppEEARS** - Application for Extracting and Exploring Analysis Ready Samples

**ArcGIS Pro** - Professional desktop GIS application from ESRI used to visualize and analyze GIS data

**ASFDAAC** - Alaska Satellite Facility Distributed Active Archive Center

**Backscatter** - Electromagnetic energy that is reflected back toward its source by terrain or particles in the atmosphere

**Band** - A layer in a raster dataset that represents data values of a specified characteristic or specified range in the electromagnetic spectrum, a single matrix of cell values

**Bare soil** - Areas lacking vegetation cover

**Beer-Lambert law** - The amount of light absorbed by a substance is proportional to its concentration and path length

**Beer-Lambert physical model** - Application of Beer-Lambert law

**Bimodal** - Distribution of data with two distinct peaks or modes

**Blue Band** - A band in the red region of the visible spectrum, 450nm to 520nm

**Canopy cover** - The proportion of forest covered by the vertical projection of tree crowns

**Clip** - Extraction of a portion of a dataset based on a specified boundary or extent

**Cloud mask** - A technique used to identify and filter out pixels in imagery that are obscured by clouds or cloud shadows

**Composite** - A combination of multiple datasets or bands into a single image, can include combining datasets across different times

**CSU** - California State University

**CWC** - Canopy Water Content, the amount of water stored within the vegetation canopy, grams of water per square meter of ground surface

**dNBR** - Differenced Normalized Burn Ratio, assess the severity of burns based on the difference between pre-fire and post-fire normalized burn ratio

**ECOSTRESS** - ISS Ecosystem Spaceborne Thermal Radiometer Experiment on Space Station

**EMIT** - International Space Station Earth Surface Mineral Dust Source Investigation

**ESI** - Evaporative Stress Index, quantifies vegetative water stress, actual evapotranspiration by potential evapotranspiration

**ET** - Evapotranspiration, the amount of water transferred from the Earth's surface to the atmosphere through evaporation and transpiration, thermal infrared sensors are used to estimate vegetative evapotranspiration

**EVI** - Enhanced Vegetation Index, used to quantify vegetation greenness and correct for atmospheric conditions and canopy background noise

**Fire severity** - Quantitative measurement of the effects a fire has on the environment, considering impacts to vegetation and soil

**Fuel** - Flammable plant material

**Full polarization** - The ability to transmit and receive electromagnetic waves both vertically and horizontally, relating to a radar system such as SAR

**GeoTIFF** - Image file format that includes embedded geospatial data for images to accurately align with real-world locations

**Green Band** - A band in the green region of the visible spectrum, 500nm to 600nm

**H** - Horizontal polarization, oscillation of an antenna's electronic field in the horizontal plane

**High severity** - Fire has completely consumed surface vegetation, the organic soil layer may be entirely burned

**HLS / HLSL-30** - Harmonized Landsat and Sentinel-2 Operational Land Imager Surface Reflectance and Top of Atmosphere (TOA) Brightness Daily Global 30m

**Invasive** - Non-native plants that when introduced to an area establish and proliferate rapidly, disrupting ecosystems by outcompeting native plants

**IRO** - Institutional Research Opportunity

**ISS** - International Space Station

**LANDFIRE** - Landscape Fire and Resource Management Planning Tools

**Large-scale/Large Fires** - Fire burning with a size and intensity in which the interaction between its own convection column and weather conditions determine its behavior

**L-band** - Data acquired by employing an electronically scanned antenna, fully polarized

**Level/L** - The degree of which data has been processed (series of operations on data) from raw to highly processed, regarding data processing

**Least squares** - Within regression analysis, a parameter estimation method made by minimizing the sum of square differences (residuals)

**Linear regression** - Estimates the linear relationship between dependent and one or more explanatory variable

**L1** - Level 1 data, raw unprocessed data

**Low severity** - Surface vegetation is lightly burned, tree canopies and organic soil layers remain mostly intact

**L2** - Level 2 data, derived geophysical variables from L1 data

**L2A** - Level 2 data, derived from geolocated instrument data, such as highest and lowest surface elevations

**L3** - Level 3 data, geophysical variables mapped on uniform space-time grid scales (averaged over time and space)

**L4** - Level 4 data, model results from lower-level data analysis which may be derived from multiple measurements

**Moderate severity** - A significant portion of surface vegetation burned away, partial scorched tree canopies, organic soil layer may have been affected

**NASA** - National Aeronautics and Space Administration

**NBR** - Normalized Burn Ratio, index used to assess the severity of burn scars

**NDVI** - Normalized Difference Vegetation Index, measures the greenness and density of vegetation using red and NIR band

**NIR** - Near Infrared, region of the electromagnetic spectrum 770nm to 900nm, infrared radiation closest to the visible spectrum

**NISAR** - NASA-IRO Synthetic Aperture Radar

**OLS** - Ordinary Least Squares, A least square method that makes assumption about the residuals such as, residuals have constant variance, residuals are uncorrelated, residuals are normally distributed

**Open tree canopy** - Areas of a forest where the crowns of the trees are not tightly packed and do not overlap to form a continuous layer

**Polarization** - The direction of travel of an electromagnetic wave including, vertical, horizontal, or circular allowing for more detailed information extraction

**Prescribed burn** - Controlled fires intentionally created and controlled by agencies to remove excess fuel

**Python** - Versatile programming language

**QA** - Quality Assurance, process or method to ensure that data meets defined quality criteria

**Raster** - A matrix of cells (pixels) organized into rows and columns, an image, in which each pixel contains a value that represents a specific attribute

**Red Band** - A band in the red region of the visible spectrum, 625nm to 740nm

**RTC** - Radiometric Terrain Correction, used to reduce distortion in imagery caused by terrain variation by ensuring backscatter values accurately reflect the surface

**Rx** - Prescribed

**SBG** - Surface Biology and Geology

**SBNF** - San Bernardino National Forest

**Shrubland** - Areas where vegetation distribution is dominated by shrubs or short trees

**Simplified regression analysis** - regression analysis using only one independent variable

**Sparse tree canopy** - Areas of forest where tree crowns are spread out, leaving space in-between crowns

**Sparse vegetation** - Areas with low vegetation cover, 10-50% vegetation surface coverage

**Spatial resolution** - A sensor's ability to register a physical object on the ground, within a single cell or pixel

**Spectral solar absorption** - The amount of solar radiation energy absorbed by a surface or object

**Surface reflectance** - Incoming solar radiation that is reflected by the Earth's surface

**SWIR** - Short-Wave Infrared, region of the electromagnetic spectrum 1400nm to 3000nm

**SWIR1** - A band in the short-wave infrared region of the electromagnetic spectrum 1550nm to 1750nm

**SWIR2** - A band in the short-wave infrared region of the electromagnetic spectrum 2090nm to 2350nm

**Temporal resolution** - The frequency at which images are captured over the same geographic area

**TOA** - Top of Atmosphere

**Transformation** - The conversion of geographic coordinates on a map or image from one system to another

**UAVSAR** - Uninhabited Aerial Vehicle Synthetic Aperture Radar

**Unburned** - Vegetation remains intact, no soil change, no evidence of fire impact

**USDA** - United States Department of Agriculture

**V** - Vertical polarization, oscillation of an antenna's electric field in the vertical plane

**Vegetation greenness** - The amount and vigor of green vegetation, often used as an indicator of plant health

**WUE** - Water Use Efficiency, the ratio of biomass produced to water consumed, gross primary production by evapotranspiration

**WUI** - Wildland Urban Interface, the zone where regions of human development meet vegetative fuels

## 7. References

- About LANDFIRE*. (n.d.). Landfire. <https://landfire.gov/about-landfire>
- About us*. (n.d.). San Bernardino Valley Municipal Water District. <https://www.sbvmd.com/about-us>
- An, K., Jones C.E., & Lou, Y. (2024). Assessment of Pre- and Post-Fire Fuel Availability for Wildfire Management Based on L-Band Polarimetric SAR. *Advancing Earth & Space Science*. <https://doi.org/https://doi.org/10.1029/2023EA002943>
- California Institute of Technology. (2023). RTC\_notebook. nasa-jpl. uavsar-wildfire-rtc/RTC\_notebook.ipynb at main · nasa-jpl/uavsar-wildfire-rtc · GitHub. <https://github.com/nasa-jpl/uavsar-wildfire-rtc>
- Carleton, T. (n.d.). *Simple derivation of omitted variables bias*. Bren School of Environmental Science & Management, UCSB, Environmental Data Science 222. [https://tcarleton.github.io/EDS-222-stats/labs/04-week-four/OVB\\_derivation.pdf](https://tcarleton.github.io/EDS-222-stats/labs/04-week-four/OVB_derivation.pdf)
- Center for geospatial science and technology*. (n.d.). CSUN, College of Social and Behavioral Sciences. <https://www.csun.edu/center-for-geospatial-science-technology>
- Cvetkovich, G. T., & Winter, P. L. (2008). *The experience of community residents in a fire-prone ecosystem: A case study on the San Bernardino National Forest* (PSW-RP-257). United States Department of Agriculture, Forest Service, Pacific Southwest Research Station. <https://doi.org/10.2737/PSW-RP-257>
- Donovan, V. M., Twidwell, D., Uden, D. R., Tadesse, T., Wardlow, B. D., Bielski, C. H., Jones, M. O., Allred, B. W., Naugle, D. E., & Allen, C. R. (2020). Resilience to large, “Catastrophic” wildfires in North America’s grassland biome. *Earth Future*, 8. <https://doi.org/10.1029/2020EF001487>
- Fire management*. (n.d.). USDA, Forest Service. <https://www.fs.usda.gov/main/sbnf/fire>
- Fusco, E. J., Finn, J. T., Balch, J. K., Nagy, R. C., & Bradley, B. A. (2019) Invasive grasses increase fire occurrence and frequency across US ecoregions. *Proc. Natl. Acad. Sci. U.S.A.*, 116 (47), 23594-23599. <https://doi.org/10.1073/pnas.1908253116>.
- Gabbert, B. (2021). NASA uses UAVs and satellites equipped with radar to monitor recovery from vegetation fires. *Wildfire Today*. <https://wildfiretoday.com/2021/02/08/nasa-uses-uavs-and-satellites-equipped-with-radar-to-monitor-recovery-from-vegetation-fires/>
- Green, R.O., Painter, T.H, Roberts, D.A., & Dozier, J. (2006). Measuring the expressed abundance of the three phases of water with an imaging spectrometer over melting snow. *AGU Water Resources Research*, 42(10). <https://doi.org/10.1029/2005WR004509>
- Jamali, S., Jönsson, P., Eklundh, L., Ardö, J., & Seaquist, J. (2015). *Detecting changes in vegetation trends using time series segmentation*. 156, 182–195. <https://doi.org/https://doi.org/10.1016/j.rse.2014.09.010>.
- Keifer, M., van Wagtenonk, J.W. & Buhler, M. (2006). Long-term surface fuel accumulation in burned and unburned mixed-conifer forests of the Central and Southern Sierra Nevada, CA (USA). *Fire Ecology*, 2, 53–72. <https://doi.org/10.4996/fireecology.0201053>

- Land Processes Distributed Active Archive Center. (2024a). 2 Working with EMIT L2A Reflectance and ECOSTRESS L2 LST Products. NASA Vitals. VITALS/python/02\_Working\_with\_EMIT\_Reflectance\_and\_ECOSTRESS\_LST.ipynb at main · nasa/VITALS · GitHub
- Land Processes Distributed Active Archive Center. (2024b). 3 Equivalent Water Thickness/Canopy Water Content from Imaging Spectroscopy Data. NASA Vitals. VITALS/python/03\_EMIT\_CWC\_from\_Reflectance.ipynb at main · nasa/VITALS · GitHub
- Lopez-De-Castro, M., Prieto-Herraez, D., Asensio-Sevilla, M. I., & Pagnini, G. (2022). A high-resolution fuel type mapping procedure based on satellite imagery and neural networks: Updating fuel maps for wildfire simulators. *ELSEVIER*, 27. <https://doi.org/10.1016/j.rsase.2022.100810>
- Martin, E. R., Gregory P. Asner, Emily Francis, Anthony Ambrose, Wendy Baxter, Adrian J. Das, Nicolas R. Vaughn, Tarin Paz-Kagan, Todd E. Dawson, Koren R. Nydick, Nathan L. Stephenson (2018). Remote measurement of canopy water content in giant sequoias (*Sequoiadendron giganteum*) during drought. *Forest Ecology and Management*, 70196693. <https://www.usgs.gov/publications/remote-measurement-canopy-water-content-giant-sequoias-sequoiadendron-giganteum-during>
- Miller, R. K., Field, C. B., & Mach, K. J. (2020). Barriers and enablers for prescribed burns for wildfire management in California. *Nature sustainability*, 3, 101–109. <https://doi.org/10.1038/s41893-019-0451-7>
- NASA EarthData. (n.d.). *Synthetic Aperture Radar (SAR)*. NASA EARTHDATA. <https://www.earthdata.nasa.gov/learn/earth-observation-data-basics/sar>
- NASA Jet Propulsion Laboratory. (n.d.). *ECOsysteM Spaceborne Thermal Radiometer Experiment on Space Station ECOSTRESS*. NASA Jet Propulsion Laboratory California Institute of Technology. <https://www.jpl.nasa.gov/missions/ecosystem-spaceborne-thermal-radiometer-experiment-on-space-station-ecostress/>
- Northwest Fire Science Consortium (2017). *NWFSC Fire Facts: What is? Topography*. Northwest Fire Science Consortium. [https://www.nwfirescience.org/sites/default/files/publications/FIREFACTS\\_Topography.pdf](https://www.nwfirescience.org/sites/default/files/publications/FIREFACTS_Topography.pdf)
- Rhew, I.C, Vander Stoep, A., Kearney, A., Smith, N.L., Dunbar, & M.D. (2011). Validation of the Normalized Difference Vegetation Index as a measure of neighborhood greenness. *Annals of Epidemiology*, 21(12), 946–952. <https://doi.org/10.1016/j.annepidem.2011.09.001>
- Roteta, E., Bastarrika, A., Franquesa, M., & Chuvieco, E. (2021). Landsat and Sentinel-2 based burned area mapping tools in Google Earth Engine. *Remote sensing*, 13(4), 816-844. <https://doi.org/10.3390/rs13040816>
- San Bernardino County. (n.d.) Data Commons. [https://datacommons.org/place/geoId/06071?utm\\_medium=explore&mprop=count&popt=Person&hl=en](https://datacommons.org/place/geoId/06071?utm_medium=explore&mprop=count&popt=Person&hl=en)
- Sapkota, R.P, Dhital, N.B., & Rijal, K. (2023). Fire-mediated biomass loss of woody species seedlings causing demographic bottleneck in the Terai Forests of Central Nepal. *Global Ecology and Conservation*, 48, e02705. <https://doi.org/10.1016/j.gecco.2023.e02705>



- Simard, M., Riel, B. V., Denbina, M. and Hensley, S. (2016). Radiometric Correction of Airborne Radar Images Over Forested Terrain With Topography. *IEEE Transactions on Geoscience and Remote Sensing*, 54(8), 4488-4500. <https://doi.org/10.1109/TGRS.2016.2543142>
- Tucker, C.J. (1979). Red and Photographic Infrared Linear Combinations for Monitoring Vegetation. *Remote Sensing of Environment*, 8, 127–150. [https://doi.org/http://dx.doi.org/10.1016/0034-4257\(79\)90013-0](https://doi.org/http://dx.doi.org/10.1016/0034-4257(79)90013-0)
- United Nations Office for Outer Space Affairs UN-SPIDER. (n.d.). Normalized Burn Ratio (NBR). <https://un-spider.org/advisory-support/recommended-practices/recommended-practice-burn-severity/in-detail/normalized-burn-ratio>
- United Nations Office for Outer Space Affairs UN-SPIDER (2018). Step by step: Burn Severity with Python and optical data (Sentinel-2). UN-SPIDER. UN-SPIDER/burn-severity-mapping-EO / burn\_severity.ipynb at main · UN-SPIDER · GitHub
- U.S. Department of Agriculture, Forest Service. (n.d.). *Angelus Oaks Understory Burn*. <https://www.fs.usda.gov/project/?project=19249>
- U.S. Department of Agriculture, Forest Service. (2021). *Research & development at a glance Fiscal Year 2021* (FS-1177). [https://www.fs.usda.gov/sites/default/files/fs\\_media/fs\\_document/RD-at-a-Glance.pdf](https://www.fs.usda.gov/sites/default/files/fs_media/fs_document/RD-at-a-Glance.pdf)
- U.S. Department of Agriculture, Forest Service. (2023). *National prescribed fire resource mobilization strategy* (FS-1216). <https://www.fs.usda.gov/sites/default/files/2023-06/Rx-Fire-Strategy.pdf>
- U.S. Department of the Interior, U.S. Geological Survey (2023). LANDFIRE Technical Documentation, U.S. Geological Survey, Reston, Virginia: 2023. <https://pubs.usgs.gov/of/2023/1045/ofr2023>
- Van Wagtendonk, J.W., Benedicts, J.M., & Sydoriak, W.M. (1998). Fuel bed characteristics of Sierra Nevada Conifers. *Western Journal of Applied Forestry*, 13(3), 73-84. <https://doi.org/10.1093/wjaf/13.3.73>
- Zhu, Y., Murugesan, S. B., Masara, I. K., Myint, S. W., & Fisher, J. B. (2024). Examining wildfire dynamics using ECOSTRESS data with machine learning approaches: The case of South-Eastern Australia's black summer. *Remote Sensing in Ecology and Conservation*. <https://doi.org/10.1002/rse2.422>

## 8. Appendices

### Appendix A: LANDFIRE

**Figure A.1**

Historical land cover changes within Fire Perimeters. *Historical vegetation precedent within the Line Fire and AOU burn perimeter in San Bernardino National Forest, San Bernardino, CA (LANDFIRE 2023).*

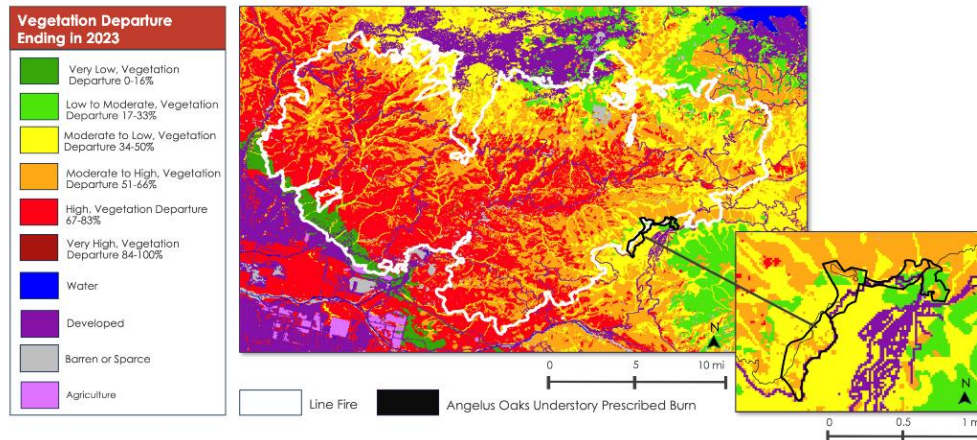


**Figure A.2**

Existing Vegetation Classes within Fire Perimeters. *Vegetation classification within the Line Fire burn perimeter in San Bernardino National Forest, San Bernardino, CA (LANDFIRE 2023).*

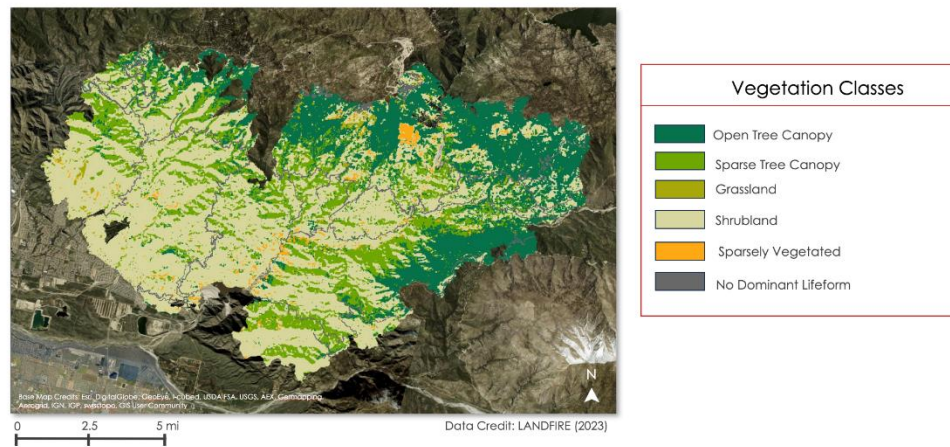
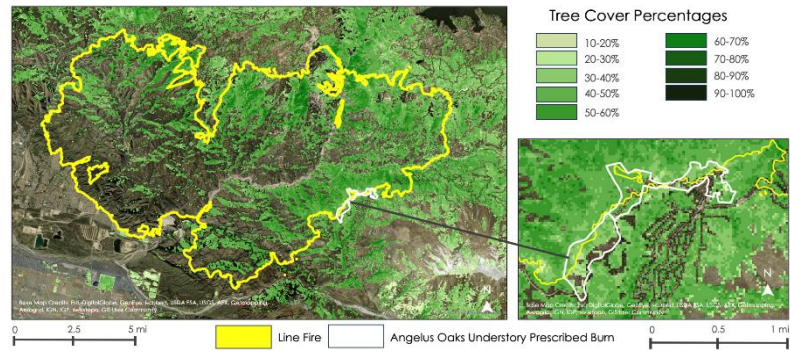


**Figure A.3**

Existing tree cover percentages within Fire Perimeters. *Canopy Cover Percentages within the Line Fire and AOU burn perimeter in San Bernardino National Forest, San Bernardino, CA (LANDFIRE 2023).*



## Appendix B: EMIT & ECOSTRESS

**Figure B.1**  
Canopy Water Content within fire perimeters estimated with ISS EMIT surface reflectance (ISS EMIT, 2023).

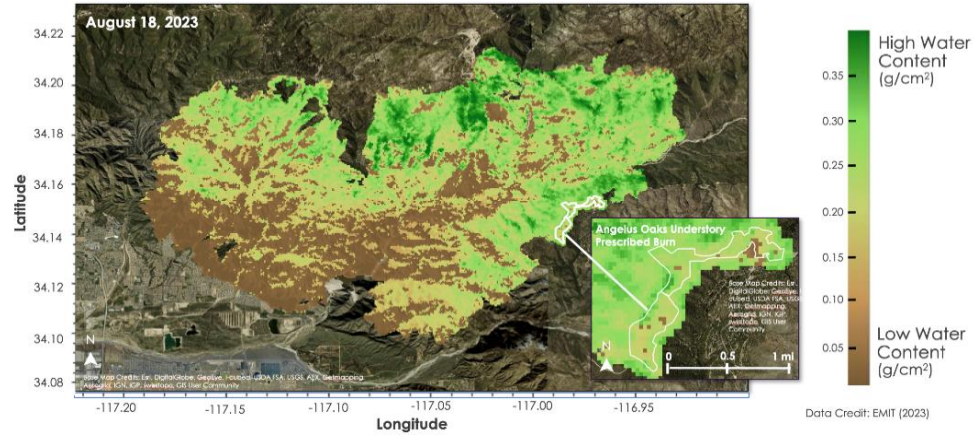


**Figure B.2**  
Histograms displaying canopy water content throughout fire extents (ISS EMIT, 2023).

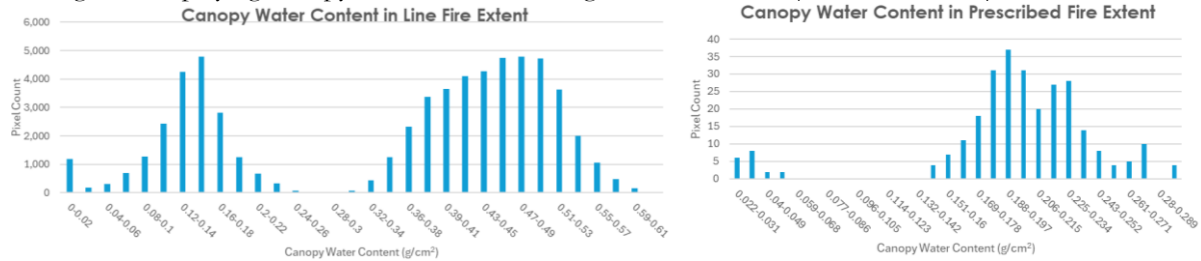
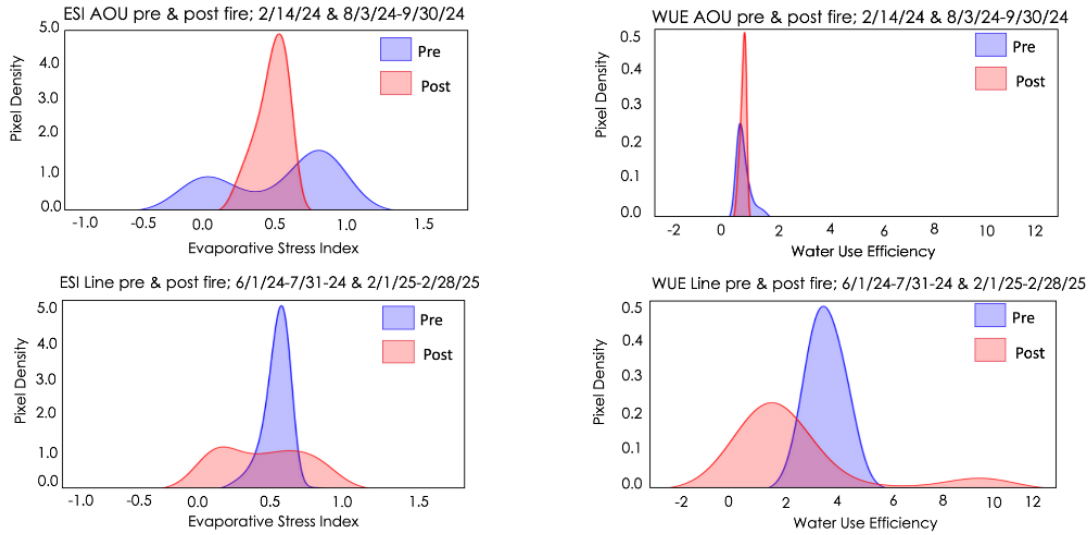


**Figure B.3**  
Histograms displaying Evaporative Stress Index and Water Use Efficiency Change pre- and post-AOU and Line fire burn (ISS ECOSTRESS, 2024).



## Appendix C: NDVI & EVI

**Figure C.1**



NDVI Landscape Greenness Trends in Line Fire extent, from September 5 – December 21, 2024 (HLS, 2024–2025).

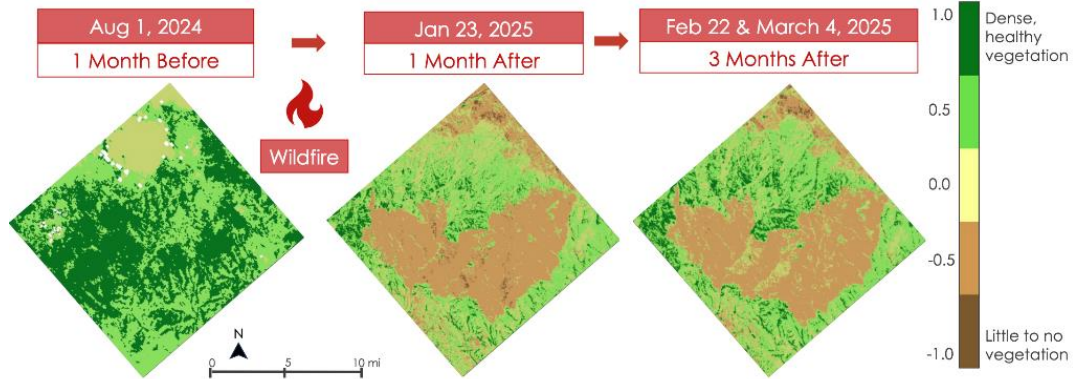
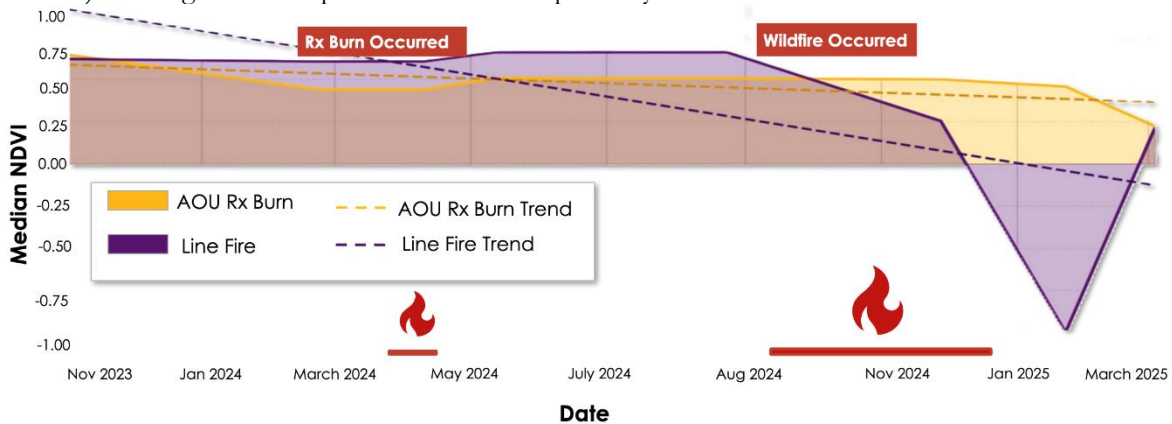


**Figure C.2**

NDVI Landscape Greenness Trends Over Time. NDVI Time Series Ordinary Least Squares (OLS) Regression Analysis: Angelus Oaks Understory Prescribed Burn vs Line Fire, from November 2023 – March 2025 (HLS, 2023–2025). The regression outputs for each fire respectively are shown below this.

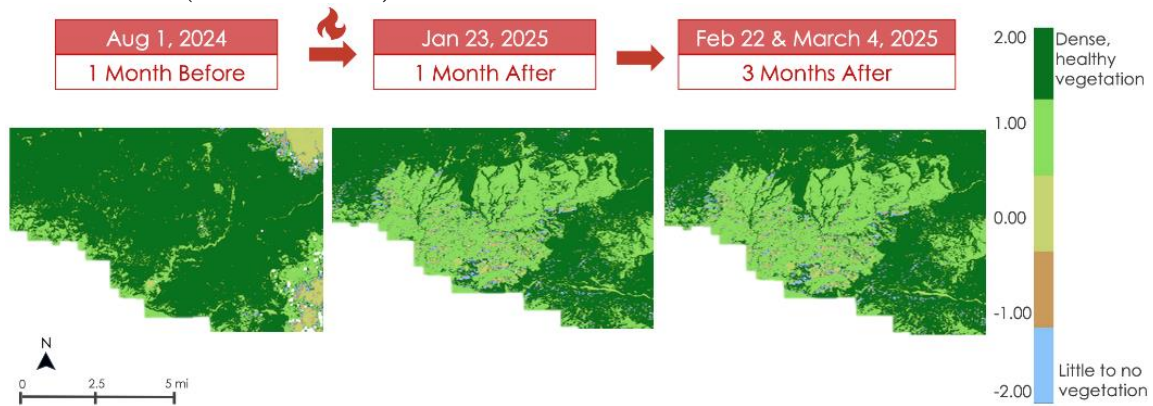


| Angelus Oaks Understory Prescribed Burn OLS Regression Summary:   |                  |                     |          |       |        | Line Fire OLS Regression Summary:   |                  |                     |          |       |        |
|---|------------------|---------------------|----------|-------|--------|---|------------------|---------------------|----------|-------|--------|
| OLS Regression Results  |                  |                     |          |       |        | OLS Regression Results  |                  |                     |          |       |        |
| Dep. Variable:  | median_ndvi      | R-squared:          | 0.435    |       |        | Dep. Variable:  | median_ndvi      | R-squared:          | 0.412    |       |        |
| Model:  | OLS              | Adj. R-squared:     | 0.354    |       |        | Model:  | OLS              | Adj. R-squared:     | 0.327    |       |        |
| Method:   | Least Squares    | F-statistic:        | 5.393    |       |        | Method:   | Least Squares    | F-statistic:        | 4.895    |       |        |
| Date:   | Sun, 16 Mar 2025 | Prob (F-statistic): | 0.0532   |       |        | Date:   | Sun, 16 Mar 2025 | Prob (F-statistic): | 0.0626   |       |        |
| Time:   | 15:40:07         | Log-Likelihood:     | 10.068   |       |        | Time:   | 15:40:07         | Log-Likelihood:     | -4.3283  |       |        |
| No. Observations:   | 9                | AIC:                | -16.14   |       |        | No. Observations:   | 9                | AIC:                | 12.66    |       |        |
| Df Residuals:   | 7                | BIC:                | -15.74   |       |        | Df Residuals:   | 7                | BIC:                | 13.05    |       |        |
| Df Model:   | 1                |                     |          |       |        | Df Model:   | 1                |                     |          |       |        |
| Covariance Type:  | nonrobust        |                     |          |       |        | Covariance Type:  | nonrobust        |                     |          |       |        |
|   | coef             | std err             | t        | P> t  | [0.025 |   | coef             | std err             | t        | P> t  | [0.025 |
| const   | 9.4987           | 3.888               | 2.443    | 0.045 | 0.304  | const   | 42.9571          | 19.251              | 2.231    | 0.061 | -2.565 |
| x1  | -0.0005          | 0.000               | -2.322   | 0.053 | -0.001 | x1  | -0.0021          | 0.001               | -2.213   | 0.063 | -0.004 |
|   |                  |                     |          |       | 0.975] |   |                  |                     |          |       | 0.000] |
| Omnibus:  | 1.552            | Durbin-Watson:      | 1.449    |       |        | Omnibus:  | 9.629            | Durbin-Watson:      | 2.249    |       |        |
| Prob(Omnibus):  | 0.460            | Jarque-Bera (JB):   | 1.007    |       |        | Prob(Omnibus):  | 0.008            | Jarque-Bera (JB):   | 3.720    |       |        |
| Skew:   | -0.587           | Prob(JB):           | 0.604    |       |        | Skew:   | -1.458           | Prob(JB):           | 0.156    |       |        |
| Kurtosis:   | 1.858            | Cond. No.           | 2.59e+06 |       |        | Kurtosis:   | 4.189            | Cond. No.           | 2.59e+06 |       |        |
| Notes:  |                  |                     |          |       |        | Notes:  |                  |                     |          |       |        |
| [1] Standard Errors assume that the covariance matrix of the errors is correctly specified  |                  |                     |          |       |        | [1] Standard Errors assume that the covariance matrix of the errors is correctly specified.   |                  |                     |          |       |        |
| [2] The condition number is large, 2.59e+06. This might indicate that there are strong multicollinearity or other numerical problems. |                  |                     |          |       |        | [2] The condition number is large, 2.59e+06. This might indicate that there are strong multicollinearity or other numerical problems. |                  |                     |          |       |        |



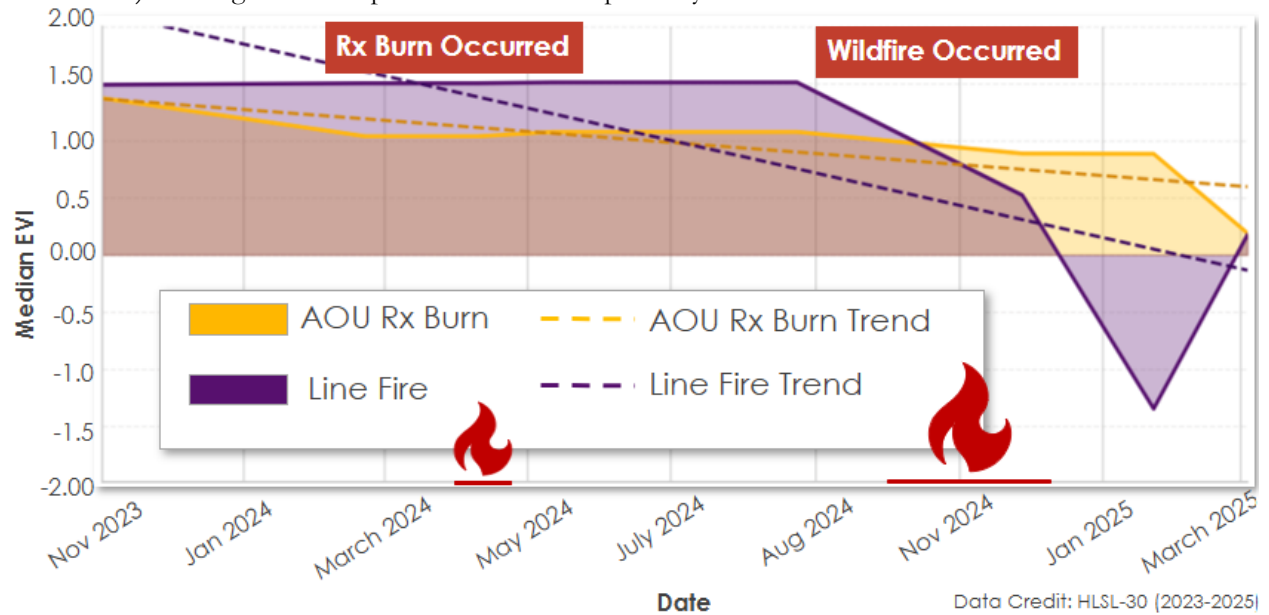
**Figure C.3**

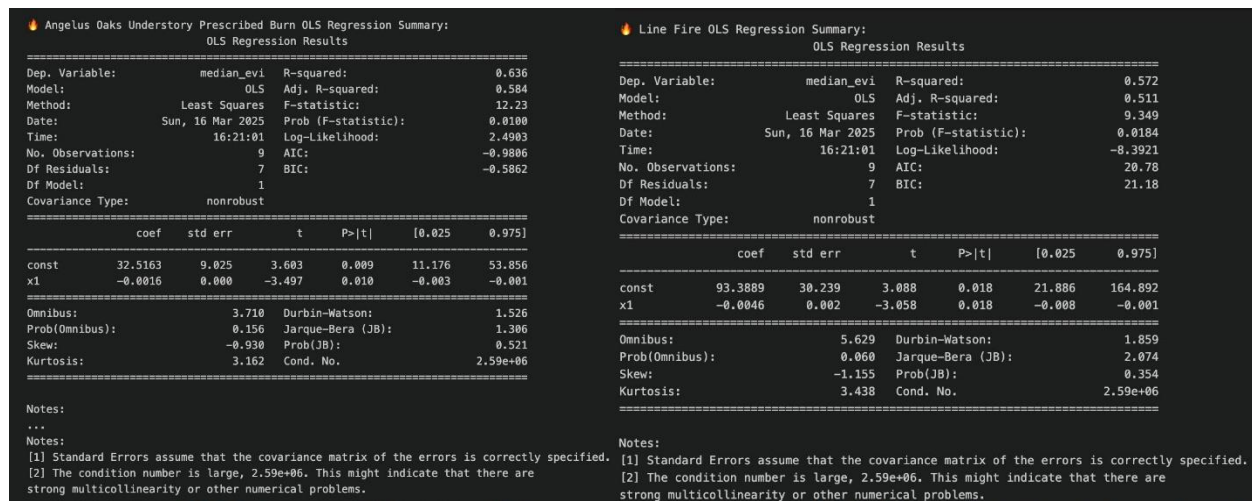
Enhanced Vegetation Index (EVI) Landscape Greenness Trends in Line Fire extent from September 5 – December 21, 2024 (HLS, 2024–2025).



**Figure C.4**

EVI Landscape Greenness Trends Over Time. EVI Time Series Ordinary Least Squares (OLS) Regression Analysis: Angelus Oaks Understory Prescribed Burn vs Line Fire, from November 2023 – March 2025 (HLS, 2023–2025). The regression outputs for each fire respectively are shown below this.





## Appendix D: Burn Severity

**Figure D.1**

Prescribed burn categorized by soil burn severity. Differenced normalized burn ratio (dNBR) in AOU extent (left) and (right) ArcGIS Basemap “Environment” AOU Prescribed Burn Elevation Topography Map (HLS, 2024–2025,). Basemap Source: Esri, TomTom, Garmin, FAO, NOAA, USGS, © OpenStreetMap contributors, © World Wildlife Fund, Inc., and the GIS User Community.

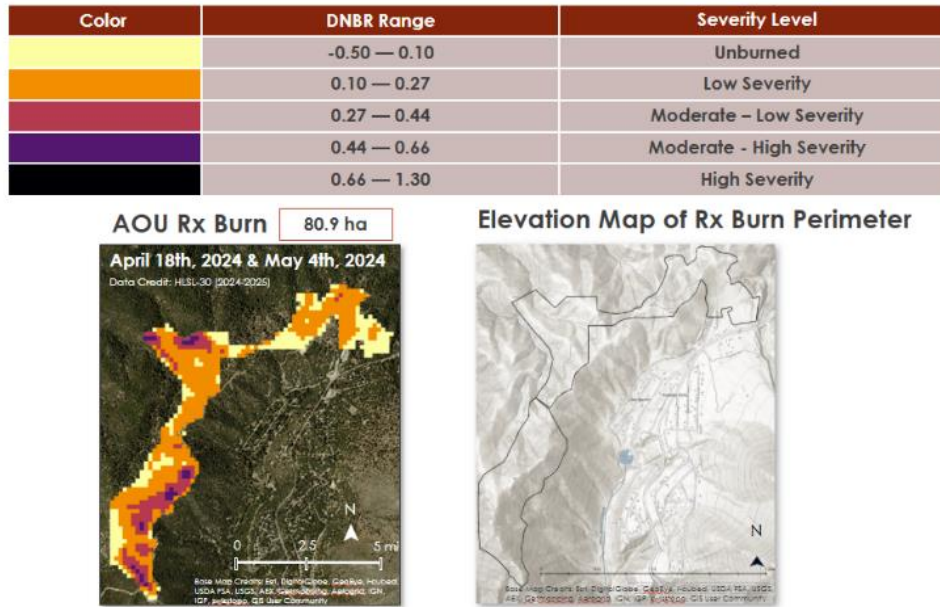


**Figure D.2**

Line Fire was categorized by soil burn severity. Differenced normalized burn ratio (dnBR) in wildfire extent (left) and (right) ArcGIS Basemap “Environment” AOU Prescribed Burn Elevation Topography Map (HLS 2024-2025, ). Basemap Source: Esri, TomTom, Garmin, FAO, NOAA, USGS, © OpenStreetMap contributors, © World Wildlife Fund, Inc., and the GIS User Community.

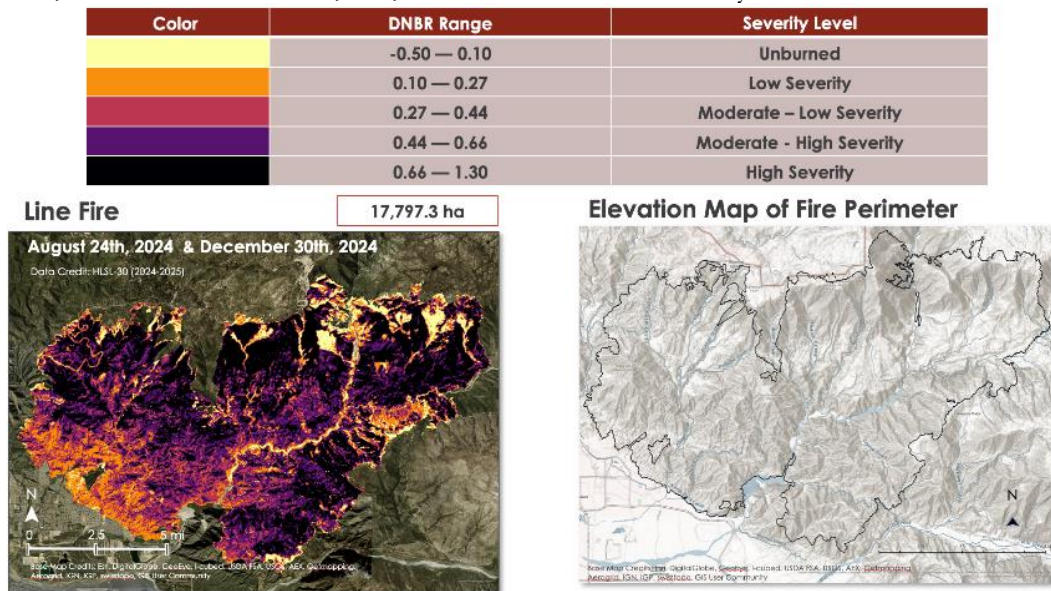


**Figure D.3**

Examining Fire Type Burn Severity Trends within the Line Fire (purple) and AOU Prescribed Burn (gold) fire perimeters by Burn Severity Classification in San Bernardino National Forest, San Bernardino, CA (HLS, 2024–2025).

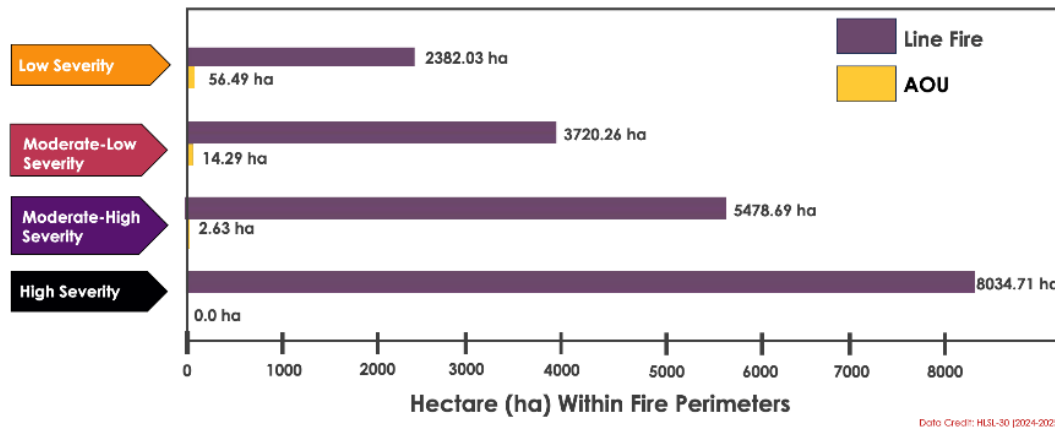


**Figure D.4**

Composite image of San Bernardino National Forest with Line Fire perimeter (purple) and AOU perimeter (black) dNBR classified soil burn severity (UAVSAR, 2023, 2025).

### Results: dNBR Validation with UAVSAR

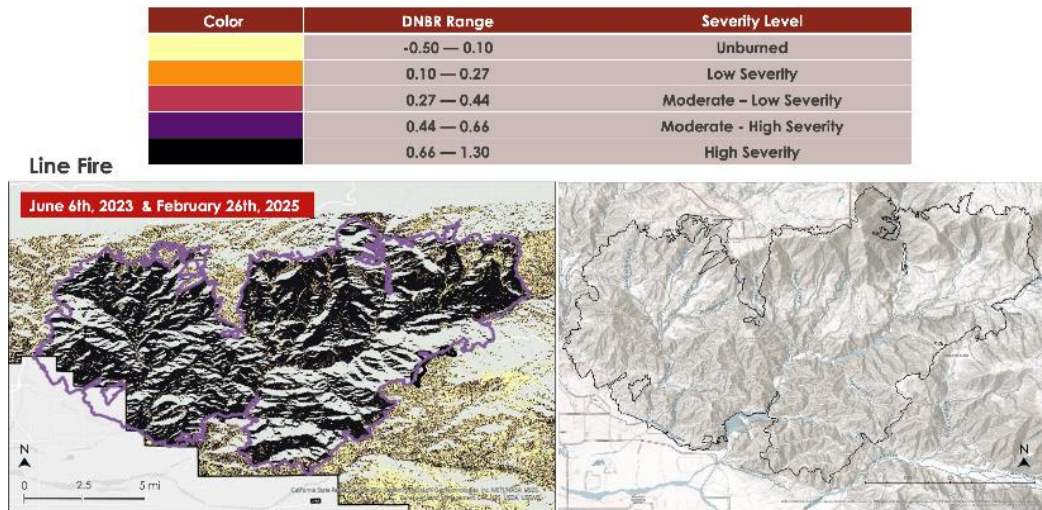
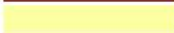






**Figure D.5**

Composite image of San Bernardino National Forest with Line Fire perimeter (purple) and AOU perimeter (black) dNBR classified soil burn severity (UAVSAR, 2023, 2025).



## Results: dNBR Validation with UAVSAR

| Color   | DNBR Range   | Severity Level           |
|---|--------------|--------------------------|
|  | -0.50 — 0.10 | Unburned                 |
|  | 0.10 — 0.27  | Low Severity             |
|  | 0.27 — 0.44  | Moderate – Low Severity  |
|  | 0.44 — 0.66  | Moderate - High Severity |
|  | 0.66 — 1.30  | High Severity            |

### Prescribed Burn

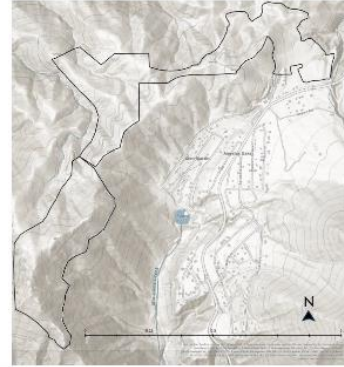
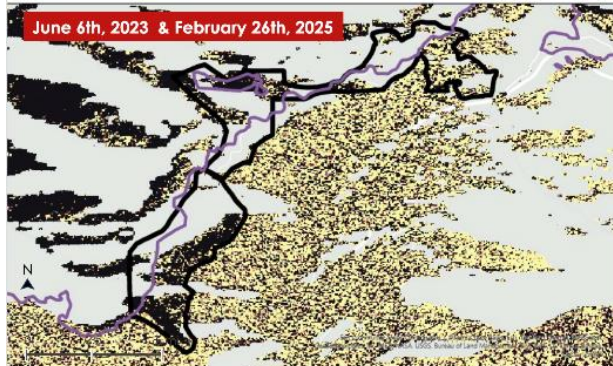




**Figure E.1**

Errors, uncertainty, and feasibility concerns. Varying spatiotemporal resolution inconsistencies were present.

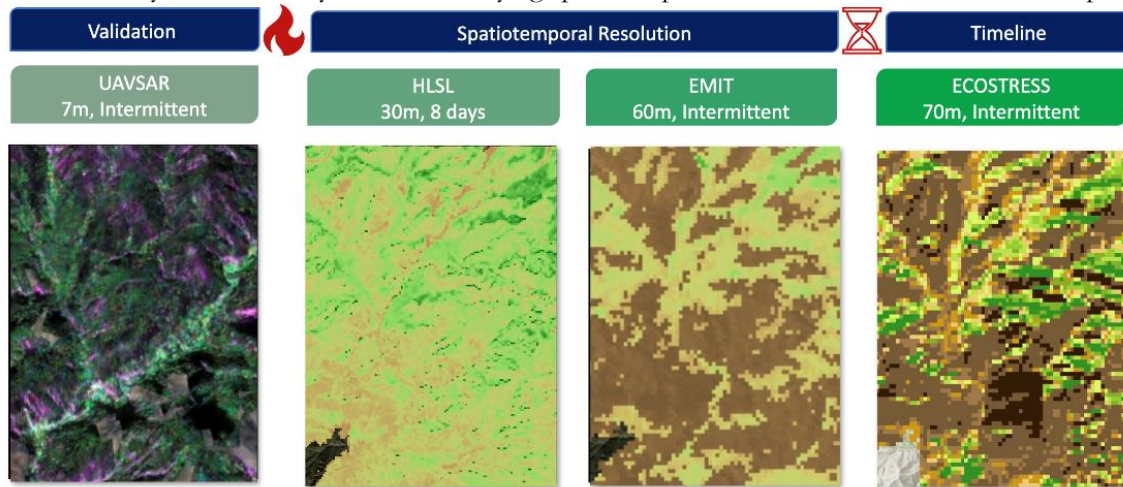


**Figure E.2**

Courtesy of the USDA Forest Service, this map shows the location of the Angelus Oaks Prescribed Fire, April 30 to May 3.

